



Automatic hippocampus localization in histological images using PSO-based deformable models

Roberto Ugolotti, Pablo Mesejo, Stefano Cagnoni, Mario Giacobini,
Ferdinando Di Cunto

► To cite this version:

Roberto Ugolotti, Pablo Mesejo, Stefano Cagnoni, Mario Giacobini, Ferdinando Di Cunto. Automatic hippocampus localization in histological images using PSO-based deformable models. 13th Genetic and Evolutionary Computation Conference companion (GECCO'11), Jul 2011, Dublin, Ireland. pp.487-494, 10.1145/2001858.2002038 . hal-01221664

HAL Id: hal-01221664

<https://inria.hal.science/hal-01221664>

Submitted on 28 Oct 2015

HAL is a multi-disciplinary open access archive for the deposit and dissemination of scientific research documents, whether they are published or not. The documents may come from teaching and research institutions in France or abroad, or from public or private research centers.

L'archive ouverte pluridisciplinaire **HAL**, est destinée au dépôt et à la diffusion de documents scientifiques de niveau recherche, publiés ou non, émanant des établissements d'enseignement et de recherche français ou étrangers, des laboratoires publics ou privés.

Automatic Hippocampus Localization in Histological Images using PSO-Based Deformable Models

Roberto Ugolotti

Dept. of Information
Engineering

University of Parma, Italy
rob_ugo@ce.unipr.it

Pablo Mesejo

Dept. of Information
Engineering

University of Parma, Italy
pmesejo@ce.unipr.it

Stefano Cagnoni

Dept. of Information
Engineering

University of Parma, Italy
cagnoni@ce.unipr.it

Mario Giacobini

Dept. of Animal Production
Epidemiology and Ecology
University of Torino, Italy

mario.giacobini@unito.it

Ferdinando Di Cunto

Molecular Biotechnology
Center

University of Torino, Italy
ferdinando.dicunto@unito.it

ABSTRACT

The Allen Brain Atlas (ABA) is a cellular-resolution, genome-wide map of gene expression in the mouse brain which allows users to compare gene expression patterns in neuroanatomical structures. The correct localization of the structures is the first step to carry on this comparison in an automatic way.

In this paper we present a completely automatic tool for the localization of the hippocampus that can be easily adapted also to other subcortical structures. This goal is achieved in two distinct phases.

The first phase, called “best reference slice selection”, is performed by comparing the image of the brain with a reference Atlas provided by ABA using a two-step affine registration. By doing so the system is able to automatically find to which brain section the image corresponds and wherein the image the hippocampus is roughly located.

The second phase, the proper “hippocampus localization”, is based on a method that combines Particle Swarm Optimization (PSO) and a novel technique inspired by Active Shape Models (ASMs). The hippocampus is found by adapting a deformable model derived statistically, in order to make it overlap with the hippocampus image.

Experiments on a test set of 120 images yielded a perfect or good localization in 89.2% of cases.

Categories and Subject Descriptors

I.5.4 [Pattern Recognition]: Applications—*Computer Vision*; I.2.10 [Artificial Intelligence]: Vision and Scene Understanding

General Terms

Algorithms, Experimentation

Keywords

Affine Registration, Hippocampus, Particle Swarm Optimization, Allen Brain Atlas, Active Shape Models, Automatic Localization

1. INTRODUCTION

The Allen Brain Atlas (ABA) project aims to bridge the divide between genomics and neuroanatomy, by providing a global approach to understanding the genetic structural and cellular architecture of the mouse brain. It contains a genome-scale collection of cellular resolution gene expression profiles obtained by means of In Situ Hybridization (ISH), performed on serial sections [1]. Using ISH, the spatial distribution of gene expression patterns (where genes are actively transcribed) can be generated throughout an entire organ or organism for thousands of genes. In particular, the ABA contains the expression patterns in the adult mouse brain of about 20,000 genes. For each gene, several images are provided, and each image is related to one reference slice, extracted from a reference Atlas composed of 132 coronal and of 21 sagittal sections.

Among the different brain structures, the hippocampal formation (HF) is a particularly interesting component of the mammalian brain. Indeed, considering the strong role of the HF in learning and memory processes [16], it is extremely important to precisely map gene expression at the cellular and subcellular level within this region. Moreover, since the hippocampal volume has turned out to be an early biomarker for Alzheimer’s disease [4], there is great interest in automated methods to accurately, robustly, and reproducibly extract the hippocampus from medical images, in order to automatize diagnostic screenings. The HF (Figure 1), composed by Hippocampus and Subiculum (SUB), is located within the medial temporal lobe. In turn, the Hippocampus is composed by Ammon’s Horn (CA) and Dentate Gyrus (DG). We present a system aimed at the automatic localization of the entire hippocampus by localizing the pyramidal (SP) and granule (SG) cell layers, which belong to the

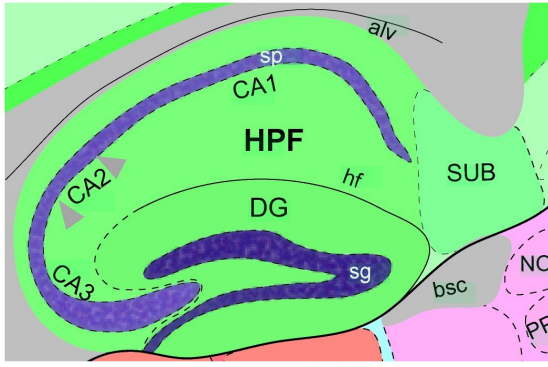


Figure 1: Regions in Hippocampal Formation

CA and DG regions, respectively.

In this work, we deal with sagittal slices of mouse brain obtained from the ABA. The main features of these images in general, and of hippocampus images in particular, are:

- presence of artifacts: tears, scraps, bubbles, streaks in tissue, partial cut off of regions;
- fuzziness of the hippocampus boundaries;
- variability of brain structure shapes;
- no relevance of color for detecting anatomical structures;
- variable resolution: high resolution regions coexist with low resolution ones;
- large image size (around 15.000x7.000 pixels, ~35MB);
- contrast variability between structures: due to the nature of gene expression patterns, different genes are not expressed equally in the same anatomical region, making it difficult to construct a consistent model for each landmark in all images. Moreover, grained patterns with many irregularities hamper the classification of individual pixels into anatomical structures based on intensity;
- orientation issues: images are rotated or displaced on the slide;
- lighting issues: within a set, some images are much brighter than others.

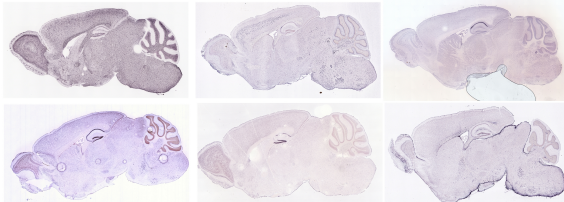


Figure 2: Examples of slices from the ABA

All these characteristics (see some examples in Figures 2 and 3) significantly increase the difficulty of operations like localization or segmentation. In this paper, we present a

fully automatic 2D localization method based on Particle Swarm Optimization, atlas-based registration and deformable models. We focus mainly on sagittal images of the brain to locate the hippocampus, but the method can be applied to coronal images, as well as to other subcortical structures. The main idea is to capture the general structure of the hippocampus, based on prior knowledge about shape, which is the most invariant element on these images. The final goal of our work is to create a tool for extracting statistics for different genes, to be able to compare automatically the levels and the spatial distribution of their expression in corresponding parts of the brain through the analysis of thousands of images. The first step of this process has to be the fine localization and segmentation of brain structures, to perform texture analysis of selected areas.

Section 2 explains the basics of the techniques we have applied and the previous work which has inspired the method we have developed. In Section 3, an overview of the system is presented, which offers a general description of the method. Section 4 gives details on the method used to select the best reference slice and Section 5 focuses on the hippocampus localization. Finally, Sections 6 and 7 present some experimental results and the conclusions, respectively.

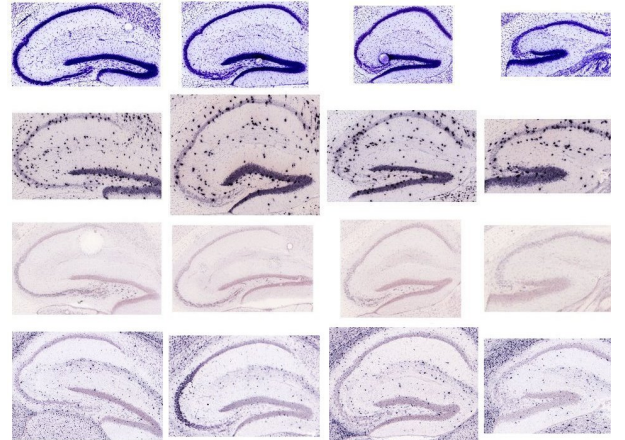


Figure 3: Hippocampus variability. Horizontal-wise images show how hippocampus sections look different in different parts of the brain. Vertical-wise, it can be seen that corresponding sections from different brains maintain some rough shape similarity.

2. BACKGROUND

This work takes advantage of the combination of several techniques, such as Particle Swarm Optimization, deformable models and image registration.

2.1 Particle Swarm Optimization

Particle Swarm Optimization (PSO) is a bio-inspired optimization algorithm introduced by Kennedy and Eberhart [11] and used for optimization of non-linear functions. It is based on the simulation of the social behaviour of bird flocks. In the last fifteen years PSO has been applied to a very large variety of problems [18] and many variants of the original algorithm have been proposed [3].

During the execution of PSO a set of particles moves within the function domain (called search space) searching

for the optimum of the function (best fitness value). The motion of each particle can be described by the following two simple equations which regulate the position and the velocity update of the particles:

$$\begin{aligned} P_n(t) &= P_n(t-1) + v_n(t) \\ v_n(t) &= w \cdot v_n(t-1) \\ &+ c_1 \cdot \text{rand}() \cdot (BP_n - P_n(t-1)) \\ &+ c_2 \cdot \text{rand}() \cdot (BGP - P_n(t-1)) \end{aligned}$$

where $P_n(t)$ and $v_n(t)$ are the position and velocity of the n^{th} particle in the present iteration, c_1 , c_2 and w (inertia factor) are positive constants, $\text{rand}()$ returns random values uniformly distributed in $[0, 1]$, BP_n is the best-fitness position visited so far by the particle and BGP is the best-fitness position visited so far by any particle of the swarm. Thus, we can say that each particle relies both on “individual” and on “swarm” intelligence.

One of the major problems with PSO is the so-called “premature convergence”, which is frequent especially when dealing with multimodal functions. If a component of the swarm finds a local optimum, other particles may converge to that point before searching other unexplored better regions of the function domain. This problem may be obviated (but in a strongly problem-dependent way) by tuning (possibly dynamically) the parameters c_1 , c_2 and w , but other different solutions have been proposed in the last years [6].

2.2 Deformable Models

Deformable models are curves or surfaces, defined within an image domain, that move under the influence of “internal” forces, related with the curve features, and “external” forces, related with the surrounding image. Internal forces keep the model smooth during deformation. External forces are defined such that the model is attracted toward an object or other features of interest. Deformable models have become a standard in medical image analysis [13].

Active Shape Models, introduced by Cootes et al [7], can be seen as a way to add prior knowledge to deformable models. These shape models represent objects by sets of labelled points selected by an expert on a set of training images. Each point is placed on a specific part of the object. By examining the statistics of the positions of the labelled points a “Point Distribution Model” is derived. The model considers the average position of the points, and the main modes of variation found in the training set. It is important to note that an instance of the model can only take into account deformations which appear in the training set: this way the model has problems with unexpected shapes, but it is robust with respect to noise and image artifacts, like missing or damaged parts.

2.3 Image Registration

Image registration is the process of finding a transformation that aligns one image to another one. The inputs are two images: a reference image, and another one, known as the target image, that can be modified to match it. The output is a geometrical transformation or mathematical mapping. This transformation can be rigid (preserving angles and distances), affine (parallel lines are preserved but not lengths and angles), or elastic (where external forces tend to minimize the deformation) [23].

2.4 Related Work

The previous work related with the system we have developed can be divided according to three main topics: brain histological image processing; automatic localization of the hippocampus and other brain structures; and Swarm Intelligence or Evolutionary Computation applied to Image Processing.

Regarding the first category, much work relates to histological image segmentation, registration and reconstruction techniques, among which we could mention: 3D reconstruction from a sequence of histological coronal 2D slices using a model built by non-linear transformations between the neighbouring slices [17]; image registration combining the high-frequency components of slice-to-slice histology registration with the low-frequency components of the histology-to-MRI registration [22]; a 2D to 3D nonlinear registration using a PDE-based registration technique driven by a local normalized-mutual-information similarity measure [9]; slice-by-slice segmentation of anatomical structures where the successful segmentation of one section provides a prior for the subsequent one [19].

Concerning the second category, most work usually deals with semi-automatic methods (in which some user interaction or seed initialization is necessary) or relates to different kind of images (like MRI) with very different characteristics. In this context there are two main tendencies (which are combined in many cases): shape models to introduce prior knowledge [10] and atlas based segmentation [5, 21].

Finally, in relation to swarm intelligence or evolutionary computation applied to image processing, a large number of known techniques have been applied. Genetic Snakes [2] are active contour models with an energy minimization procedure based on Genetic Algorithms (GAs). In [14], GAs are applied to evolve a population of shapes, using prior shape knowledge to produce feasible deformations while also controlling the scale and localization of these deformations. Scatter Search, in [8], is used to solve the registration matching problem. Finally, Particle Swarm Optimization has been successfully applied to road sign detection [15], considering a set of key points representative of the shape and colors of the object.

3. OVERVIEW OF THE SYSTEM

The goal of automatically extracting statistical information about gene expression in brain structures (in this case, the hippocampus in sagittal brain slices) can be achieved in four main steps:

1. Best Reference Slice Selection. The Sagittal Atlas of the ABA comprises 21 labelled reference slices, carrying information related to the position of brain structures. Determining which slice is the most similar to a target image allows one to refer to the corresponding model of the structure of interest. This step is particularly important for the hippocampus because hippocampi of different brains have huge variability in size and shape (see Figure 3). Along with the selection of the most suitable reference slice, the Region of Interest (ROI) which is most likely to contain the particular anatomical structure is extracted by using the coordinates of the Atlas;
2. Structure Localization. This stage refines the rough

- localization of the structure of interest obtained in the previous one;
3. Segmentation. In this phase the external and internal boundaries of the localized structure are precisely defined. For instance, the hippocampus is composed by several sub-regions (CA1, CA2, CA3, sg, sp and DG) which need to be identified to perform texture analysis accurately;

4. Texture Analysis. Textural information about the different regions is extracted, in order to get some quantitative values that define the genomic state of the tissue. The system output is a vector of features for each gene which allows one to cluster genes into similar subsets.

This work presents only the first two steps, which define an accurate, automatic and fast structure localization system. The Best Reference Slice Selection has been implemented as a two-step affine registration method (see Section 4). The Hippocampus Localization uses a PSO-based Deformable Model approach, in which each particle of PSO is a hippocampus model (see Section 5). For the optimization of the parameters of both operations we designed and used an improved PSO algorithm which limits, as far as possible, premature convergence and stagnation. This is very important because the fitness functions we are going to deal with are strongly multimodal.

3.1 Proposed PSO

Two main features differentiate our PSO algorithm from the original one. The first has been suggested by Liu et al [12]. Instead of using a static inertia factor w , they adapt its value to the fitness function of each particle. In particular, if the objective is to minimize the fitness value, the so-called adaptive inertia weight factor (AIWF) is determined as follows:

$$w = \begin{cases} w_{min} + \frac{(w_{max}-w_{min}) \cdot (f-f_{min})}{f_{avg}-f_{min}} & \text{if } f \leq f_{avg} \\ w_{max} & \text{if } f > f_{avg} \end{cases}$$

where w_{max} and w_{min} denote the maximum and minimum possible values of w , f is the current fitness of the particle, f_{avg} and f_{min} are the average and minimum fitnesses of all particles of the swarm, respectively. This way, w varies depending on a particle's fitness so that good particles tend to perform exploitation to refine results by local search, while bad particles tend to further explore the search space.

The second change with respect to the original algorithm is the re-initialization of a particle in case of stagnation. When a particle can not improve its best position in a preset number of iterations, it moves to a random direction with very high velocity:

$$\begin{aligned} v_n(t) &= k \cdot randn() \\ P_n(t) &= P_n(t-1) + v_n(t) \end{aligned}$$

where $k > 1$ is a constant and $randn()$ returns random values from a Gaussian distribution. This way, the search performed by PSO privileges exploration of the search space to reduce the probability of falling into a local optimum.

4. BEST REFERENCE SLICE SELECTION

The first step of the localization process consists of finding the correct position of the target image within the brain. As

explained above, this is an important preliminary stage that greatly influences the following steps.

The position of an image is selected according to the similarity between the image itself and the ABA reference images. In order to define what “similar” means in this context, we must take into account that intensity and color are not relevant, while much more important is the likeness between the global shape of the two brains and, as we have shown, between the shapes of the hippocampi.

To find the best reference slice, we use a two-step method (summarized in Figure 4) that considers the similarity between the global shape of the brains and of the two hippocampi. The only piece of a-priori knowledge we use is that the position of the hippocampus is broadly the same in every brain and that all the hippocampi have roughly the same shape.

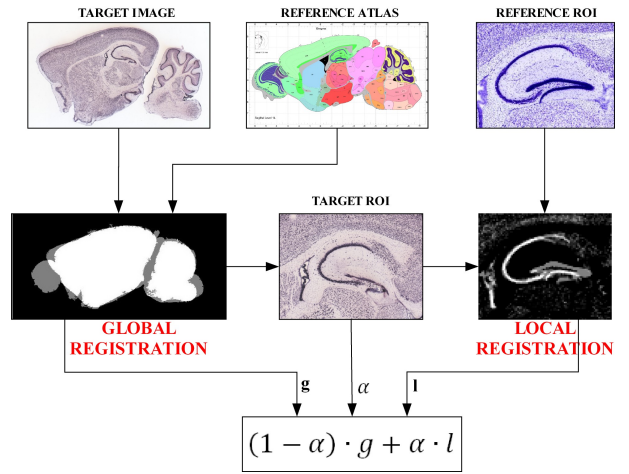


Figure 4: Best Reference Slice Selection: Data Flow

The first step performs an affine registration between the target image and each one of the Atlas references. Affine registration is a widely used technique for reconstructing and matching medical images since it can usually reach a good trade-off between quality and computational effort.

We base the affine registration only on the shape of the two brains. This means that the images downloaded from the ABA are first segmented and binarized before registration to obtain a binary image that is white where the brain is visible (foreground) and black elsewhere (background).

After the global registration, we extract the region of the target image that falls within the coordinates of the ROI which contains the reference hippocampus. We assume that, at this point, the hippocampus of the target image is entirely or partially included in the extracted ROI, and that SP and SG are among the brightest regions of the ROI. Then, an equalization process is performed to reduce the differences between the images, and we start a local affine registration process, in which we expect to match the two hippocampi.

After these two registration steps, we have two measures that represent the similarity between the target image and each reference image:

- the first one, g_k , is the squared difference between the binarized target and the binarization of the k^{th} reference brain slice;

- the second one, l_k , is the squared difference between the hippocampus regions in the two images.

The reference image that minimizes the following fitness function (see Figure 4) is selected as best slice:

$$f_k = (1 - \alpha) \cdot g_k + \alpha \cdot l_k$$

where $\alpha \in (0, 1)$ is a parameter that depends on the “quality” of the extracted ROI. A good quality ROI is an image where the anatomical parts of the hippocampus are clearly visible. We observed that good images can be distinguished from bad ones by simply looking at the standard deviation of the intensity levels of the image: bad images usually have small standard deviations and vice versa. Accordingly, we set α to be proportional to the standard deviation of the ROI. In this way images in which the hippocampus is not clearly visible (and consequently may cause a bad local registration) do not influence the results of slice selection.

The output of this phase consists of the region of the target image where the hippocampus is expected to be found and the estimated position of the image within the brain. This also indicates which are the best models to use for the localization, ranked by similarity.

5. HIPPOCAMPUS LOCALIZATION

The use of prior knowledge for tasks like localization and object recognition considerably increases the quality of results. For instance, Mussi et al [15] perform road signs detection with a simple but effective algorithm. They search within an image using a model which has the same shape as the signs to be found. A model is composed by three sets of points: for danger signs one lies just outside the external border (therefore, on the image background), one on the external red band and one on the central white area. Then, an affine registration is applied to the model and the histograms of each transformed set of coordinates are computed; a sign is detected when the histograms of the first two sets of points are as different as possible, the histogram of the points in the red band is as different as possible from the one computed on the inner part of the sign and the histogram of the set on the red band resembles as much as possible a reference histogram centered on the red hue.

For the detection and localization of the hippocampi we adapt Active Shape Models to this approach. While in standard ASMs external forces are driven by the contours on the image, in our case we force the model’s shape to resemble as much as possible the shape of the hippocampus region we want to locate.

A substantial difference between hippocampus and road sign localization is the great variability of colors and shapes, even in the same slice (see Figure 3), which makes it impossible to define the reference histogram of a “standard” hippocampus. The only common information we have about all the hippocampi is that they have two main parts (SG and SP) which have roughly the same shape and are surrounded by lower-intensity pixels.

For this reason, we pre-process the ROIs produced by the procedure described in Section 4 to magnify the contrast between SG, SP and the rest of the hippocampus. This step is performed by saturating the brighter 65% of the image (that we suppose to contain only background) and the darker 5%; then we rescale the remaining over the entire intensity range and perform a binarization of the image with

a dynamic threshold.

5.1 Template Models

For every slice of the reference Atlas two template models (one for SG, one for SP) have been created by manually selecting the points from a training set which includes 5 to 12 images for each reference slice. A template model does not refer to the absolute position of the points, but to the relative positions (or shifts) between consecutive points in polar coordinates. This way the template model is more robust to the variation of position, shape and size among different hippocampi. Every template model is composed of two parts:

- an inner set of points that lies on the anatomical part we want to locate;
- an outer set of points that lies just outside. It is described by a rigid shift of the previous set.

A template model is described by four $2 \times n$ matrices, where n is the number of the points of the template model:

$$\mathbf{M} = \begin{bmatrix} \rho_{m1} & \vartheta_{m1} \\ \rho_{m2} & \vartheta_{m2} \\ \vdots & \vdots \\ \rho_{mn} & \vartheta_{mn} \end{bmatrix} \quad \Delta = \begin{bmatrix} \Delta_{\rho 1} & \Delta_{\vartheta 1} \\ \Delta_{\rho 2} & \Delta_{\vartheta 2} \\ \vdots & \vdots \\ \Delta_{\rho n} & \Delta_{\vartheta n} \end{bmatrix}$$

$$\mathbf{L} = \begin{bmatrix} \rho_{l1} & \vartheta_{l1} \\ \rho_{l2} & \vartheta_{l2} \\ \vdots & \vdots \\ \rho_{ln} & \vartheta_{ln} \end{bmatrix} \quad \mathbf{U} = \begin{bmatrix} \rho_{u1} & \vartheta_{u1} \\ \rho_{u2} & \vartheta_{u2} \\ \vdots & \vdots \\ \rho_{un} & \vartheta_{un} \end{bmatrix}$$

where \mathbf{M} is the “best model” and represents the standard coordinates of the inner set, Δ is the displacement of the outer set with respect to the inner set, \mathbf{L} and \mathbf{U} are the minimum and maximum values of every parameter that forms the inner set. It should be noticed that ρ_1 and ϑ_1 represent the positions of the first point with respect to the upper left corner of the image. Proceeding row-wise, every (ρ, ϑ) pair represents the position of a point with respect to the previous one.

A model, during its evolution, will tend to keep itself as similar as possible to the best model \mathbf{M} and its deformations will range within the “boundary models” \mathbf{L} and \mathbf{U} .

The matrices \mathbf{M} , \mathbf{L} and \mathbf{U} have been computed during the manual selection of the points from the training set. The first one is calculated as the median of the selected shifts and the other two are the minimum and the maximum values observed in training, respectively. To improve the template models, a manual refinement of the parameters has been performed. The matrix Δ has been manually built based on the observation of several hippocampi.

The models used for the localization of SP and SG are composed by 8 and 7 points respectively. A description of the models used for reference slice 15 is shown in Figure 5.

5.2 Fitness function

The fitness function has three components: external energy E , internal energy I and contraction factor C :

$$F = E - (I + C)$$

The external forces try to move (and deform) the model to maximize the intensity of pixels in the inner set and minimize the intensity of pixels in the outer set. For both of them

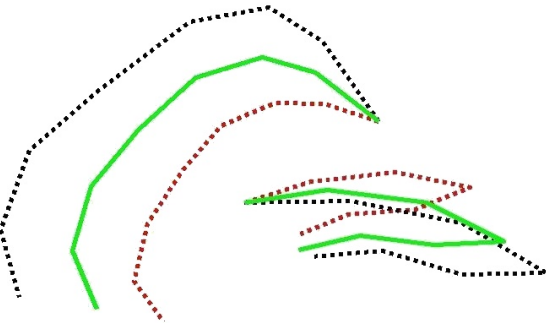


Figure 5: Best model (solid line) and boundary models (dashed lines) for SP and SG in slice 15.

we evaluate the intensity of the image within a 3×3 neighbourhood N_3 of all points in the model (Punctual Energy, PE) and in p intermediate points that lie on the segment between two consecutive points (Continuous Energy, CE).

$$PE = \sum_{i=1}^n [T(N_3(I_i)) - T(N_3(O_i))]$$

where n is the number of points in the model, $I_i = \{x_k, y_k\}$ is a point of the inner set (in cartesian coordinates), $O_i = \{x_k + \Delta x_k, y_k + \Delta y_k\}$ is a point of the outer set, $T(P)$ is the intensity of the image in P if P is a point, or the average intensity if P is a neighbourhood and $\Delta x_k, \Delta y_k$ are the elements of Δ in cartesian coordinates.

$$\begin{aligned} CE &= \sum_{i=2}^n \sum_{j=1}^p T(I_{i-1} + \frac{j}{p+1}(I_i - I_{i-1})) \\ &- \sum_{i=2}^n \sum_{j=1}^p T(O_{i-1} + \frac{j}{p+1}(O_i - O_{i-1})) \end{aligned}$$

In our case we set $p = 20$. The first shift (which actually represents the starting position of the model) was not used to keep the model independent of the localization in the image. The final external energy is computed as

$$E = \gamma_P \cdot PE + \gamma_C \cdot CE$$

where γ_P and γ_C were set to 5 and 1 respectively.

The next step is to compute the internal energy I , or those forces that reduce the deformation of the model.

$$I = \xi_\rho \cdot \sqrt{\sum_{i=2}^n (\rho_i - \rho_{bi})^2} + \xi_\vartheta \cdot \sqrt{\sum_{i=2}^n (\vartheta_i - \vartheta_{bi})^2}$$

where ξ_ρ and ξ_ϑ are two positive parameters that weight the deformation ability of the model. The higher their values, the more the model will tend to fit the best model \mathbf{M} .

The contraction factor C depends on the deformation of the model and is defined as follows:

$$C = \xi_c \cdot \|I_n - I_1\|$$

If $\xi_c < 0$ the two extremes of the model repel each other, if $\xi_c > 0$ they attract each other. In our case we set $\xi_c > 0$ for the SP models and $\xi_c < 0$ for SG models. Figure 6 shows the importance of the contraction factor.

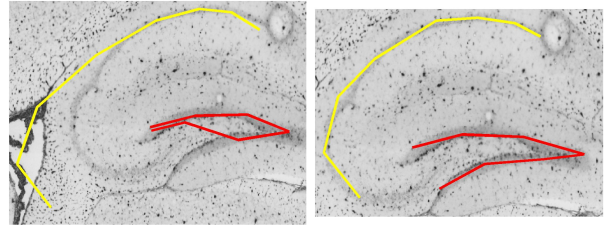


Figure 6: Two localizations of the same hippocampus with the same model and the same parameters, except for the contraction factor. On the left ξ_c is 0 for both models, on the right it was set to 0.12 for the SP model and -0.07 for the SG model.

6. EXPERIMENTAL RESULTS

For testing the system we selected images located within 10 slices of the reference Atlas (from slice 9 to 18). For every slice, four images that have that slice as reference have been chosen for a total of 40 test images. The images have been selected randomly within subsets which represent good sample of all possible hippocampi, featuring high and low levels of gene expression, good quality and low quality, and so on. Tests were run on a computer equipped with a 64-bit Intel® Core™ i7 CPU running at 2.67 GHz with 4 Gb of RAM.

6.1 Optimization Methods Comparison

Our first goal is to demonstrate that PSO in general, and the proposed variant in particular, is good at managing this kind of problems. Tables 1 and 2 show the fitness values of the localization of SP and SG, respectively, obtained by using the model relative to the reference slices suggested by ABA. We compare four different optimization methods. For every method we ran 50 tests for every image for a total of 2000 experiments. The methods used for testing are:

- Genetic Algorithm;
- Scatter Search with local search based on simulated annealing;
- PSO with linearly decreasing inertia as proposed by Shi and Eberhart [20];
- the PSO version proposed in section 3.1.

The PSO parameters for global registration were set to $w_{min} = 0.2$, $w_{max} = 1.0$, $c_1 = c_2 = 2.05$. The swarm was composed by 80 particles and was run for 300 iterations. The parameters were selected starting from the most commonly used and refined during system development.

Table 1: Comparative Results of SP Localization.

Method	Average	Std Deviation	Paired t-test
GA	108.1460	15.3365	3.05E-4
Scatter Search	87.3281	20.6248	<1.00E-16
Original PSO	110.2262	14.2808	0.2856
Modified PSO	109.6110	8.3123	-

The third column of each table indicates the average standard deviation of fitness over the single experiment repetitions. They show that the proposed PSO is more reliable than the other methods, including original PSO, because

Table 2: Comparative Results of SG Localization.

Method	Average	Std Deviation	Paired t-test
GA	140.6531	11.5352	<1.00E-16
Scatter Search	127.7413	14.5662	<1.00E-16
Original PSO	141.5991	9.3224	<1.00E-16
Modified PSO	145.2641	4.8102	-

it falls in local optima less often. An ANOVA test proved the existence of differences between the result sets, where at least one sample mean was significantly different from the others. After that, the paired Student's t-test was performed, with a level of confidence $\alpha=0.05$, for the Null Hypothesis that there are no differences between the modified PSO and the other methods. The obtained p-values (see last column of Tables 1 and 2) refute the Null Hypothesis confirming that significant differences exist between the performance of the method we propose and the other ones. The only exception is in the localization of SP, in which both PSOs achieve similar results.

6.2 Overall System Performance

In this section we report results of the entire system. The best way to evaluate the hippocampus localization is by visual observation. We divided results into three classes:

1. Perfect match: all points of the two models are on the corresponding parts and cover them almost entirely;
2. Good Localization: (i) all points of the two models are on the parts to detect but they do not cover them entirely or (ii) at most two points are slightly outside;
3. Error: all other possibilities, from three or more misplaced points to models which are located in a completely different position of the brain.

At the end of the PSO-based localization, we perform a local search to improve the results. This is made simply by re-evaluating the function, but only within a neighbourhood of size 5x5 around the points found. Our experimental results show that this helps to slightly improve the localization with very low computational effort. This improvement is due to the fact that, in this search, the points are considered independent from one another, while in the proposed model every point localization depends on all previous ones.

Table 3 summarizes the results of localization. In the actual system, we try up to three different models (according to the similarity ranking computed in the best reference slice selection) and select the one with the best fitness. We ran three tests for every image. Figure 7 shows some hippocampi with the calculated models superimposed.

Table 3: Results of Hippocampus localization.

Evaluation	Occurrences
Perfect	58 (48.3%)
Good	49 (40.9%)
Error	13 (10.8%)

Regarding time complexity, the average and standard deviation of a single experiment duration are 129s and 18s respectively. This time includes the whole process performed sequentially, from reading images to writing output to disk.

7. CONCLUSIONS

We have introduced a system for fast, accurate and completely automatic localization of subcortical structures in histological images, a problem that has been rarely discussed in the literature. We accomplished this goal in two phases. The first phase roughly locates the structure by comparing the image of the brain with images taken from the ABA reference Atlas. In the second phase, the structure is more precisely localized using a method that combines Particle Swarm Optimization and a novel technique inspired by Active Shape Models. One of the main difficulties of the system is having to deal with very variable, as well as severely damaged, images in many cases. Despite this, using the hippocampus as target structure, it has been localized with perfect or good precision in the 89.2% of cases.

8. ACKNOWLEDGMENTS

This work was funded by Compagnia di San Paolo, Torino, Italy (Programma Neuroscienze). Pablo Mesejo is funded by the European Commission (MIBISOC Marie Curie Initial Training Network, FP7 PEOPLE-ITN-2008, GA n. 238819).

9. REFERENCES

- [1] Allen Institute for Brain Science. Allen Reference Atlases. <http://mouse.brain-map.org>, 2004-2006.
- [2] L. Ballerini. Genetic snakes for color images segmentation. In *Applications of Evolutionary Computing*, volume 2037 of *Lecture Notes in Computer Science*, pages 268–277. Springer Berlin / Heidelberg, 2001.
- [3] A. Banks, J. Vincent, and C. Anyakoha. A review of Particle Swarm Optimization. Part I: background and development. *Natural Computing*, 6:467–484, 2007.
- [4] J. Barnes, J. W. Bartlett, L. A. van de Pol, C. T. Loy, R. I. Scahill, C. Frost, P. Thompson, and N. C. Fox. A meta-analysis of hippocampal atrophy rates in Alzheimer’s disease. *Neurobiology of Aging*, 30(11):1711 – 1723, 2009.
- [5] O. T. Carmichael, H. A. Aizenstein, S. W. Davis, J. T. Becker, P. M. Thompson, C. C. Meltzer, and Y. Liu. Atlas-based hippocampus segmentation in Alzheimer’s disease and mild cognitive impairment. *NeuroImage*, 27:979–990, 2005.
- [6] M. Clerc. Stagnation analysis in Particle Swarm Optimization or what happens when nothing happens. Technical Report CSM-460, Department of Computer Science, University of Essex, 2006. Edited by Riccardo Poli.
- [7] T. F. Cootes, C. J. Taylor, D. H. Cooper, and J. Graham. Active shape models-their training and application. *Comput. Vis. Image Underst.*, 61:38–59, 1995.
- [8] O. Cordón, S. Damas, and J. Santamaría. A fast and accurate approach for 3D image registration using the scatter search evolutionary algorithm. *Pattern Recognition Letters*, 27(11):1191 – 1200, 2006.
- [9] S. Gefen, N. Kiryati, and J. Nissanov. Atlas-based indexing of brain sections via 2-D to 3-D image registration. *IEEE Transactions on Biomedical Engineering*, 55(1):147 –156, 2008.
- [10] A. Ghanei, H. Soltanian-Zadeh, and J. Windham. A deformable model for hippocampus segmentation:

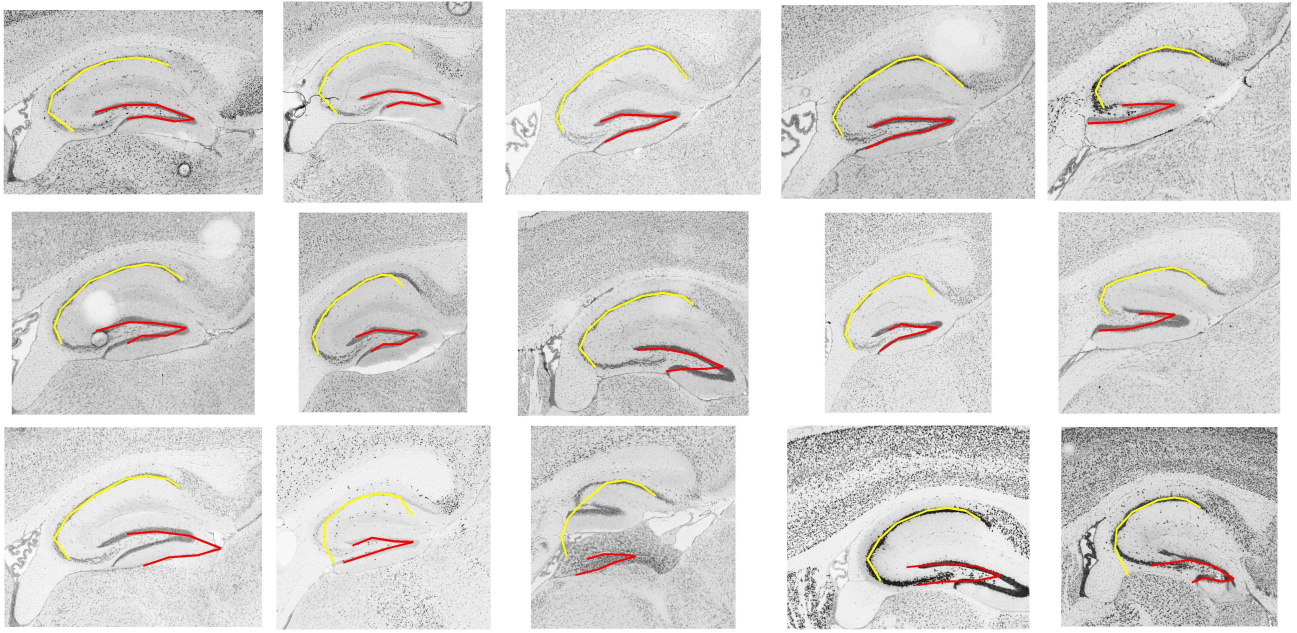


Figure 7: Some results of the localization phase. The upper row shows perfect matches, the middle row good localizations and the lower row some errors. The ROIs are selected by the process described in Section 4.

- improvements and extension to 3D. In *IEEE Nuclear Science Symposium*, volume 3, pages 1797–1801, 1996.
- [11] J. Kennedy and R. Eberhart. Particle Swarm Optimization. In *Proceedings of IEEE International Conference on Neural Networks*, volume 4, pages 1942–1948, 1995.
 - [12] B. Liu, L. Wang, Y.-H. Jin, F. Tang, and D.-X. Huang. Improved Particle Swarm Optimization combined with chaos. *Chaos, Solitons & Fractals*, 25(5):1261–1271, 2005.
 - [13] T. McInerney and D. Terzopoulos. Deformable models in medical image analysis: a survey. *Medical Image Analysis*, 1(2):91–108, 1996.
 - [14] C. McIntosh and G. Hamarneh. Evolutionary deformable models for medical image segmentation: A genetic algorithm approach to optimizing learned, intuitive, and localized medial-based shape deformation. In *Genetic and Evolutionary Computation: Medical Applications*, pages 46–67. John Wiley & Sons Ltd, 2010.
 - [15] L. Mussi, S. Cagnoni, E. Cardarelli, F. Daolio, P. Medici, and P. Porta. GPU implementation of a road sign detector based on particle swarm optimization. *Evolutionary Intelligence*, 3:155–169, 2010.
 - [16] K. A. Norman. How hippocampus and cortex contribute to recognition memory: revisiting the complementary learning systems model. *Hippocampus*, 20(11):1217–1227, 2010.
 - [17] A. Osokin, D. Vetrov, and D. Kropotov. 3-D Mouse Brain Model Reconstruction from a Sequence of 2-D Slices in Application to Allen Brain Atlas. In *Computational Intelligence Methods for Bioinformatics and Biostatistics*, volume 6160 of *Lecture Notes in Computer Science*, pages 291–303. Springer Berlin / Heidelberg, 2010.
 - [18] R. Poli. Analysis of the publications on the applications of particle swarm optimisation. *J. Artificial Evolution and Applications*, pages 1–10, 2008.
 - [19] T. Riklin-Raviv, N. Sochen, N. Kiryati, N. Ben-Zadok, S. Gefen, L. Bertand, and J. Nissanov. Propagating distributions for segmentation of brain atlas. In *4th IEEE International Symposium on Biomedical Imaging: From Nano to Macro, 2007 (ISBI'07)*, pages 1304–1307, 2007.
 - [20] Y. Shi and R. Eberhart. Empirical study of Particle Swarm Optimization. In *Proc. Congress on Evolutionary Computation (CEC'99)*, volume 3, pages 1945–1950, 1999.
 - [21] F. van der Lijn, T. den Heijer, M. M. Breteler, and W. J. Niessen. Hippocampus segmentation in MR images using atlas registration, voxel classification, and graph cuts. *Neuroimage*, 43:708–720, 2008.
 - [22] P. Yushkevich, B. Avants, L. Ng, M. Hawrylycz, P. Burstein, H. Zhang, and J. Gee. 3D mouse brain reconstruction from histology using a coarse-to-fine approach. In *Biomedical Image Registration*, volume 4057 of *Lecture Notes in Computer Science*, pages 230–237. Springer Berlin / Heidelberg, 2006.
 - [23] B. Zitová and J. Flusser. Image registration methods: a survey. *Image and Vision Computing*, 21:977–1000, 2003.